

On Reducing ShuffleNets' Block for Mobile-based Breast Cancer Detection Using Thermogram: Performance Evaluation

Rizka Ramadhana¹, Khairun Saddami², Khairul Munadi³, Fitri Arnia⁴

^{1,2,3,4} Master Program of Electrical Engineering, Universitas Syiah Kuala, Indonesia

¹ Department of Computer Science, Universitas Almuslim, Indonesia

^{2,3,4} Department of Electrical and Computer Engineering, Universitas Syiah Kuala, Indonesia

^{3,4} Telematics Research Center (TRC), Universitas Syiah Kuala, Indonesia

Article Info

Article history:

Received Aug 8, 2022

Revised Dec 3, 2022

Accepted Dec 10, 2022

Keywords:

Thermal based cancer
Early breast cancer detection
Pre-trained models
Mobile-based CNN

ABSTRACT

In this paper, we proposed a reduced-block-Shufflenet (RB-ShuffleNet) for thermal breast cancer detection. RB-ShuffleNet is a modification of Shufflenet obtained by reducing blocks from the original architecture. The images for training and testing were obtained from Database for Mastology Research (DMR). First, we detected and cropped the image based on the region of interest (ROI), in which the ROI is determined by using the red intensity profile. Then, the ROI images were trained using RB-ShuffleNets. In the experiments, we built eight architectures, based on ShuffleNet, each with a different number of reduced blocks. The result showed that RB-Shufflenet with four reduced blocks had fewer than 50% of the learning parameters of the original Shufflenet, without compromising its performance. The RB-ShuffleNet with up to four reduced blocks could achieve 100% testing accuracy. Furthermore, The RB-ShuffleNets performed better than MobileNetV2 and resulted in higher accuracy when fed with ROI images. Due to its light structure and good performance, we recommend RB-ShuffleNet as mobile-based CNN model which is preferable to implement in breast cancer detection.

Copyright © 2022 Institute of Advanced Engineering and Science.
All rights reserved.

Corresponding Author:

Fitri Arnia,
Department of Electrical Engineering,
Universitas Syiah Kuala,
Banda Aceh, Indonesia
Email: f.arnia@unsyiah.ac.id

1. INTRODUCTION

Breast cancer is one of the leading causes of death in women. Each year, new cases increase by more than 20% [1]. Early detection of breast cancer is a solution to save many women's lives. Therefore, research in this direction has become the main concern in recent years. Early detection can be done by examining breast cancer using various popular methods, one of which is thermography. Thermography is a safe, radiation-free, non-contact, and painless detection method [2], [3]. Manual detection of breast cancer is a common practice of physician or radiologist [1].

To assist physicians in cancer detection, researchers in computer vision and artificial intelligence develop automatic detection algorithms using deep learning. The previous success of deep learning in detection and classification motivates a further exploration of deep learning performance in breast cancer detection. A specific type of deep learning that is frequently used for breast cancer detection is convolutional neural networks (CNN). This is because CNN could learn the image feature, and proved the accuracy is higher than other machine learning models in breast cancer detection [4]. Currently, CNN has been used to detect breast cancer based on thermal images [3], [5], [6]. The work in [3] compared six CNN models, and among the models, ResNet 34 and ResNet50 resulted in blind accuracy validation of 100%. The work in [5] showed that

image segmentation followed by CNN could reach 100% testing accuracy. Classification has also been done in [6], which shows that CNN with Adam optimizer results in the accuracy of 98% and 95% for static and dynamic images respectively. In [7], ResNet and DenseNet reach 100% accuracy in static images. Those results showed that CNN with its deep structure succeeded in breast cancer detection. However, it requires an extensive computational process [8] for training, due to the number of datasets and parameter learning.

Meanwhile, the rapid evolution of mobile applications and devices has impacted the field of health engineering, particularly health detection tools, such as mobile-based detection of blood pressure and blood glucose. Not like the personal computer, only limited computational source is available for training in mobile devices [9]. Thus, to enable the deep learning technology to adapt to the restriction of mobile-based detection tools, the computational burden (to train) must be reduced, one is by designing and implementing the lightweight CNN. Previously, lightweight CNN for mobile devices has been proposed, like MobileNet, MobileNetV2, ShuffleNet, and ShuffleNetV2, SqueezeNet, NasNet-A-Mobile [10]–[16]. They were designed particularly for mobile devices with limited computational budget but promising a high accuracy. One approach to obtain light-weight CNN is by reducing the computational blocks of the existing deep learning structure, such as the one in [17] and [12].

Breast cancer classification using two lightweight models i.e. MobileNetv2 and ShuffleNet had been done in [7], which showed that ShuffleNet requires less training time than MobilenetV2. In addition, original ShuffleNet can perform classifications for maximum of 1000 classes. We are interested in (1) obtaining a light-weight CNN with lesser training time than the original ShuffleNet, and (2) classifying a two-class problem, normal (healthy) thermal breast image and abnormal (cancerous) thermal breast image. Therefore, we aim at investigating the impact of reducing the ShuffleNet blocks on the classification accuracy of the two-class problem. We consider that reducing some blocks of the original ShuffleNet, would not affect its classification accuracy. The contributions of this work are (1) we showed that taking out up to four basic blocks in ShuffleNet structure could be done without reducing its classification accuracy (2) we confirmed that segmented images could improve classification accuracy with faster training time, (3) we demonstrated that reducing the size of ShuffleNet architecture, thus reducing the learning parameter, could be done without compromising the performance of the CNN.

2. PROPOSED RESEARCH METHOD

The material in this research is breast thermal images obtained from the Database for Mastology Research (DMR) downloaded from Visual Lab (<http://visual.ic.uff.br/dmi>). We obtained the data based on computer simulations. The research step is shown in Figure 1. First, we collected the breast thermal images from the DMR, then we detect the ROI from those original images. Next, we classified the original and ROI breast images using our proposed convolutional neural networks, as well as current CNNs, which are MobileNet and ShuffleNet. Finally, we examined the classification results based on several common metrics.



Figure 1. Simulation pipeline of ShuffleNets Block for Mobile-based Breast Cancer Detection

2.1. Dataset Preparation

For simulation purposes, we prepared and pre-processed breast thermal images from the Database for Mastology Research (DMR), downloaded from the Visual Lab (<http://visual.ic.uff.br/dmi>). From the DMR, we used 2962 images for training, consisting of 627 images from cancerous category, and 2335 images from normal category. For testing, we used 330 images, consisting of 33 cancerous images, and 297 normal images. All those images were resized into 224×224 pixels to accommodate the restriction in ShuffleNet architecture. The ratio of training and testing images was about 9:1.

2.2. ROI Extraction

ROI is one of the processes to determine the object and separate it to the new image. Therefore, ROI will leave the required parts in the image and eliminate the parts that are not relevant. CNN will learn fewer areas after ROI detection. ROI detection has been done in thermal images, one of them is Gradient Vector Flow, which initialized the elliptical point as pre-processing with curvature function, and used CNN for classification [5]. This work demonstrates that segmentation followed by CNN classification could achieve 100% classification accuracy. ROI segmentation also had been done in [18] for thermal images with cropping, resizing, and breast normalization. The result is up to 98% accuracy using optimization of hyperparameter in

CNN. The work in [19] stated that the breast cancer detection system will be more effective by selecting the region of interest in the image.

Intensity profile had been used for several detection purposes such as crack detection [19] and early breast cancer detection [20]. In [19], the intensity profile was used to manually indicate/detect any cancerous symptom in breast tissue. In this research, we performed a simple ROI detection for removing unexpected part or region from the thermal images using the red intensity profile. It is appropriate to segment the ROI of breast thermal images based on red intensity profile, because cancerous breast frequently has dominant red intensity.

Fig. 2 shows the ROI detection method on breast thermogram using an intensity profile, in which Fig. 6(a) illustrate the position of candidate ROI. Intensity profile of an image is a collection of RGB (red–green–blue) intensity values in rows or columns [19]. Here, we consider the red intensity profile value because red is most often appears in the suspected breast image with cancer. First, the Y coordinate was determined manually based on the size of the image. The coordinates Y1 and Y2 are the upper and lower part of the breast. Based on our experiments on the images used in the simulation, we found that the best value of Y1 is about $0.95 \times$ height of the image and Y2 is about $0.4 \times$ height of the image. Then, X coordinates will be determined in the image based on the red intensity profile shown in Fig. 2(b), which is the intensity profile generated based on line Y2. Location of the X1 coordinate on the left side is determined when the red profile reaches a value > 50 , while the location of the X2 at the right is determined when the red intensity value reaches a value < 20 . The intersection area of those four coordinates is the Region of Interest (ROI).

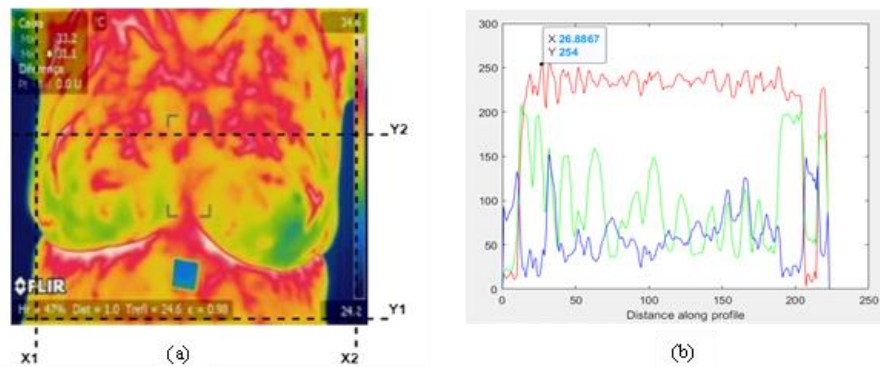


Figure 2. ROI detection method using intensity profile: (a) the border lines of ROI, (b) Intensity profile value at line Y2

2.3. Classification

Deep learning is a popular technique for automatic classification, which contain more layers than machine learning. Convolutional Neural Network (CNN), as a subsection of Deep Learning, has become the leading model for image classification. Multi layers in CNN could process nonlinear information for feature extraction and transformation in image classification [21]. CNN architectures had been expanded to many models such as Alexnet, GoogLeNet, Resnet, Inception, GoogLeNet, VGG, and so on [1], [22]. It is also popular for being able to detect and classify diseases in images, like breast cancer.

The original ShuffleNet architecture based on 16 building blocks as shown in Fig 3, where SB is ShuffleNet block. Each block consists of group convolution layers, depthwise convolution layer, and also channel shuffle operation inside. The layers arrangement in this block is shown in Fig 3. Design block building ShuffleNet consists of different layers from MobileNet which makes ShuffleNet faster in training progress.

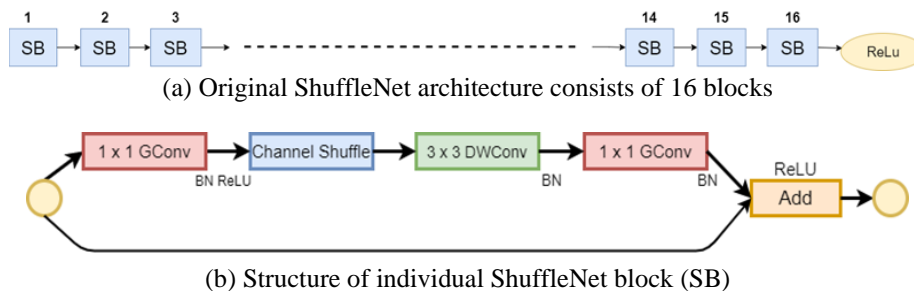


Figure 3. Architecture of original ShuffleNet and its individual building blocks

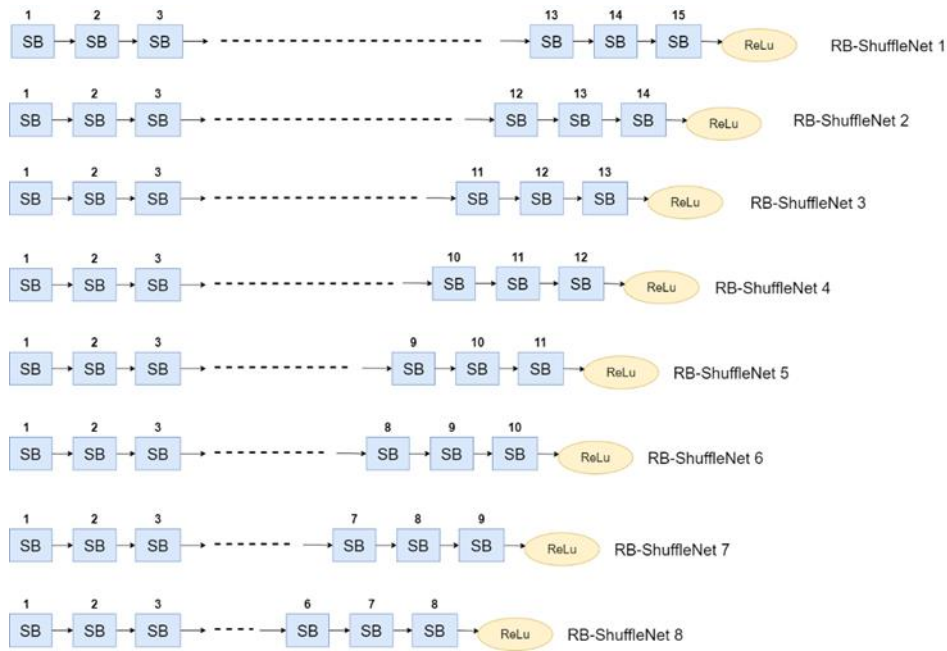


Figure 4. The method to reduce the ShuffleNet blocks to obtain the RB-ShuffleNet

ShuffleNet was designed for 1000 classes. However, cancer detection only needs two classes. Therefore, reducing several last blocks of ShuffleNet architecture is a reasonable idea. Figure 4 illustrates the method of reducing the ShuffleNet block. Based on the original ShuffleNet architecture, we remove the last block, maintaining 15 blocks, and we called this as RB-ShuffleNet 1. Then we repeat this procedure until we have eight reduced models. Each model was then trained and tested to classify the original thermal breast image and ROI of thermal breast image. We train all eight models with three different epochs, 20, 30, and 40. The performances of each reduced model in terms of accuracy as well as sensitivity and specificity were calculated and compared. Then we select models that have the best trade-off between the number of removing blocks and the accuracy value. We also compare RB-ShuffleNet models with original ShuffleNet and MobileNet.

For training purposes, we used Stochastic Gradients Descents with Momentum (SGDM) as the optimizer. SGDM is a method for updating weight in each layer using gradient information and setting the initial learning rate to 10^{-3} , and the momentum value of SGDM is 0.9. In the experiment, we set the L2 regularization of 10^{-4} . L2 Regularization was applied to penalize large weight value and to prevent higher model variance. In this paper, we used cross-entropy as the loss function.

2.4. Performance Evaluation

For experimental purposes, the dataset is divided into training, validation, and testing with a composition of 80:10:10. The testing result is evaluated using accuracy, recall, precision, and F-measure. Equation (1), (2) and (3) are the formulation of accuracy, sensitivity, and Specificity [23]:

$$Accuracy = \frac{TP+TN}{TP+TN+FP+FN} \quad (1)$$

$$Sensitivity = \frac{TP}{TP+FN} \quad (2)$$

$$Specificity = \frac{TN}{TN+FP} \quad (3)$$

where TP is true positive, which indicates the cancer image and predicted as a cancer image. TN is true negative, which indicates the healthy image and predicted successfully as a healthy image. FP is false positive, which means the healthy.

3. RESULTS AND DISCUSSION

3.1. Detection of ROI Using Red Intensity Profile

Fig. 5 shows the results of ROI detection in breast thermal images using the red intensity profile. The upper row shows the original breast thermal image, and the lower row shows the ROI of the original image after the red intensity profile is applied. The original image has the bar color (right side of the image), and some text objects. It also includes irrelevant areas such as neck and stomach. The result of ROI image could localize the breast area, excluding most of the text objects and the bar color. Removing those areas means that unwanted information is reduced and could improve classification results.

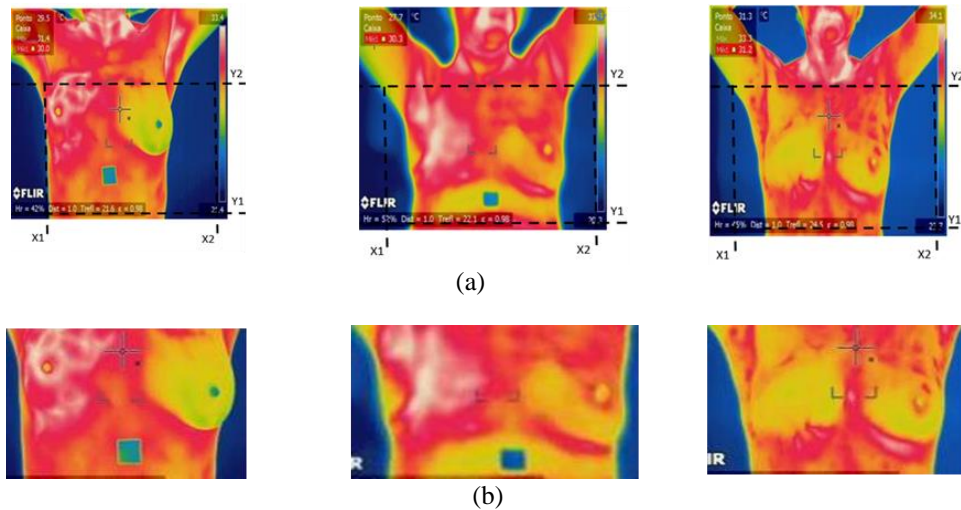


Figure 5. Segmentation of ROI image, where: (a) Original image from the database (b) extracted ROI with red profile intensity

3.2. Classification

3.2.1. RB-ShuffleNet

Tables 1, 2, and 3 showed the training and testing results of the RB-ShuffleNet on original images and ROI images respectively. Table 1 showed that as the epoch increases, the ROI image classifications resulted in slightly higher. The training result in table 1 showed RB-ShuffleNet training accuracy and time learning the model. It showed the accuracy almost close between original and ROI images. Nevertheless, training time on ROI images is consistently faster than the original images. This is possible to happen because the size of ROI image is smaller than the original image. Although only 1-3 minutes faster, it contributes to improve the model in training time.

Table 1. Training accuracy of RB-ShuffleNet

	Epoch 20		Epoch 30		Epoch 40		Epoch 30		Epoch 40		Epoch 40	
	Original Image		ROI		Original Image		ROI		Original Image		ROI	
	Acc	Time (min)	Acc	Time (min)	Acc	Time (min)	Acc	Time (min)	Acc	Time (min)	Acc	Time (min)
RB-ShuffleNet 1	0.98	23	0.98	22	0.99	35	0.98	33	0.99	47	0.99	45
RB-ShuffleNet 2	0.97	21	0.97	20	0.98	33	0.99	31	0.98	41	0.99	41
RB-ShuffleNet 3	0.97	20	0.97	19	0.97	30	0.98	29	0.98	39	0.98	39
RB-ShuffleNet 4	0.96	18	0.97	17	0.97	28	0.97	26	0.98	35	0.98	35
RB-ShuffleNet 5	0.96	15	0.96	15	0.97	26	0.97	26	0.98	35	0.98	32
RB-ShuffleNet 6	0.95	14	0.96	15	0.96	22	0.96	21	0.96	30	0.97	28
RB-ShuffleNet 7	0.94	14	0.95	13	0.96	21	0.96	19	0.97	26	0.97	26
RB-ShuffleNet 8	0.94	13	0.94	11	0.95	19	0.95	18	0.96	24	0.96	22

Table 2 showed the classification accuracy testing on original images, for all epochs, particularly using ShuffleNet structure with one up to four blocks removed (RB-ShuffleNet-1 up to RB-ShuffleNet-4). The

testing accuracy did not reach 100% on original images using RBShuffleNet. It showed in table 2, the value of sensitivity and specificity could not reach 100%. It affects the accuracy that could not reach 100%, which means there is misclassified in the model.

Table 2. Testing result using original image

	Epoch 20			Epoch 30			Epoch 40		
	Sens	Spec	Acc (%)	Sens	Spec	Acc (%)	Sens	Spec	Acc (%)
RB-ShuffleNet 1	1	0.99	99.69	1	0.99	99.69	1	0.99	99.69
RB-ShuffleNet 2	1	1	100	1	0.99	99.69	0.96	1	99.69
RB-ShuffleNet 3	0.96	0.96	99.39	1	0.99	99.69	0.96	1	99.69
RB-ShuffleNet 4	1	0.99	99.69	1	1	100	1	0.99	99.69
RB-ShuffleNet 5	1	0.99	99.69	1	0.99	99.69	0.96	1	99.69
RB-ShuffleNet 6	1	0.99	99.69	0.97	1	99.69	1	0.99	99.69
RB-ShuffleNet 7	1	0.99	99.09	0.96	0.99	99.39	1	0.99	99.69
RB-ShuffleNet 8	1	0.95	95.45	1	0.99	99.09	1	0.99	99.69

Table 3 showed the classification accuracy testing on ROI images. The obtained parameters same as in table 2. However, RB-ShuffleNet works better in ROI images. The accuracy testing showed 100% from RB-ShuffleNet 1 – RB ShuffleNet 4 in the two highest epoch. ROI images improve the work of RB-ShuffleNet in increasing accuracy testing. Other RBShuffleNet models obtain fewer score accuracy.

Table 3. Testing result using ROI image

	Epoch 20			Epoch 30			Epoch 40		
	Sens	Spec	Acc (%)	Sens	Spec	Acc (%)	Sens	Spec	Acc (%)
RB-ShuffleNet 1	1	1	100	1	1	100	1	1	100
RB-ShuffleNet 2	1	1	100	1	1	100	1	1	100
RB-ShuffleNet 3	1	1	100	1	1	100	1	1	100
RB-ShuffleNet 4	1	0.99	99.69	1	1	100	1	1	100
RB-ShuffleNet 5	1	0.99	99.69	0.97	1	99.69	0.97	1	99.69
RB-ShuffleNet 6	0.91	1	99.09	0.97	1	99.69	0.97	1	99.69
RB-ShuffleNet 7	0.88	1	98.79	1	0.99	99.39	1	0.996	99.69
RB-ShuffleNet 8	1	0.96	96.66	1	0.98	98.78	1	0.99	99.09

For convenience, Fig. 6 shows the comparison accuracy testing of RB-ShuffleNet on original and ROI thermal images, which are extracted from Tables 2 and 3. This comparison shows that RB-ShuffleNet on ROI images resulted in either the same or higher classification accuracy –with a few exceptions– than testing on original breast thermal images. For ROI images, the graphic shows that epoch=40 resulted in more stable higher accuracy than those at epoch=20 and epoch=30.

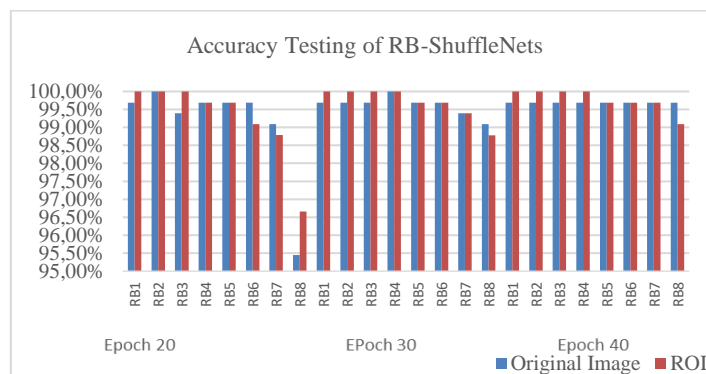


Figure 6. RB-ShuffleNet testing result on original and ROI thermal images.

3.2.2. Comparison RB-ShuffleNet with ShuffleNet dan MobileNet

To assess the performance of the RB-ShuffleNet with benchmarking CNNs, we compare the training time extracted from table 1. We also added training time from MobileNetV2 and ShuffleNet as a comparison to RB-ShuffleNet. Training time for ROI images is faster than the original image applies to all deep learning models in fig 7. This training time indicates the learning process of deep learning models. RBShuffleNet could provide faster training time than other mobile-based deep learning models, such as MobileNetV2 and ShuffleNet.

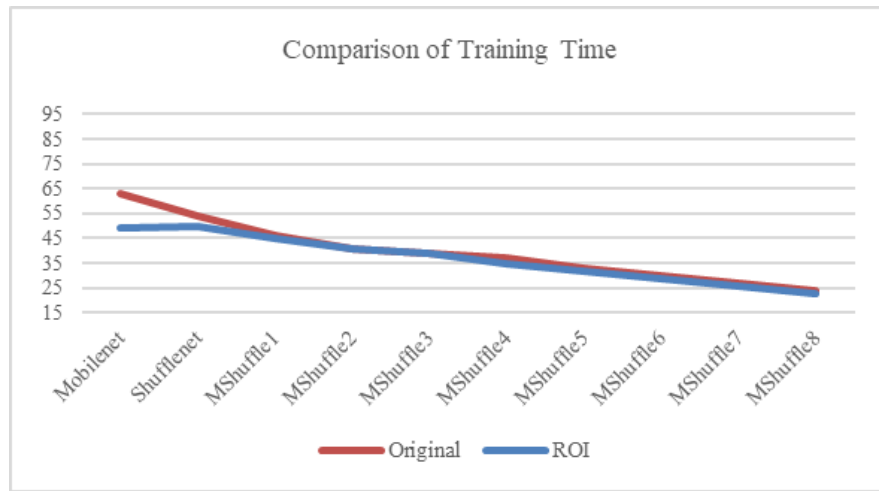


Figure 7. Training time comparison in deep learning model

In fig 8, we compare the performance of MobileNet and ShuffleNet. The figure represents the testing accuracy of deep learning model for both original and ROI breast thermal images. While the accuracy of MobileNet and ShuffleNet are the highest as expected, reaching up to 100% accuracy, the accuracy of RB-ShuffleNet1 up to ShuffleNet4 is also comparably high for ROI images which shows 100% accuracy. This evidence showed the power of RBShuffleNet using ROI images performed better than using original images. Furthermore, applying ROI images to ShuffleNet and MobileNetV2 showed the same performance as the original images. This result showed that ROI image has a positive impact on improving the performance of RB-ShuffleNet. Although fig 6 and fig 8 showed similar accuracy, the accurate medical tests is important to avoid errors, unnecessary suffering and expense [24] in breast cancer detection. Therefore, the model should obtain the maximum accuracy in testing. True and false data of mobile-based deep learning model was compared in fig 9 using confusion matrix.

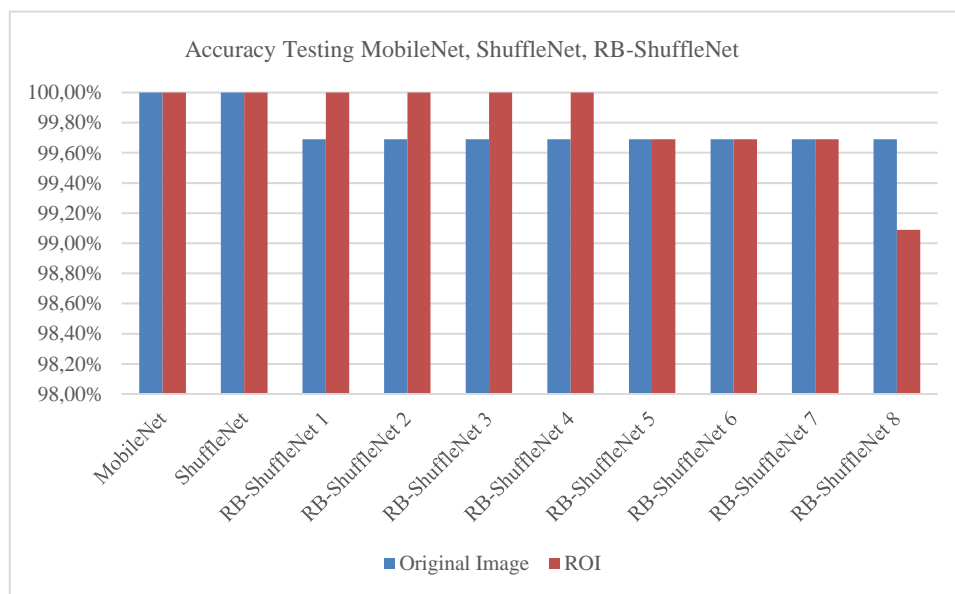


Figure 8. Testing Results of MobileNetV2 ShuffleNet and RB-ShuffleNet

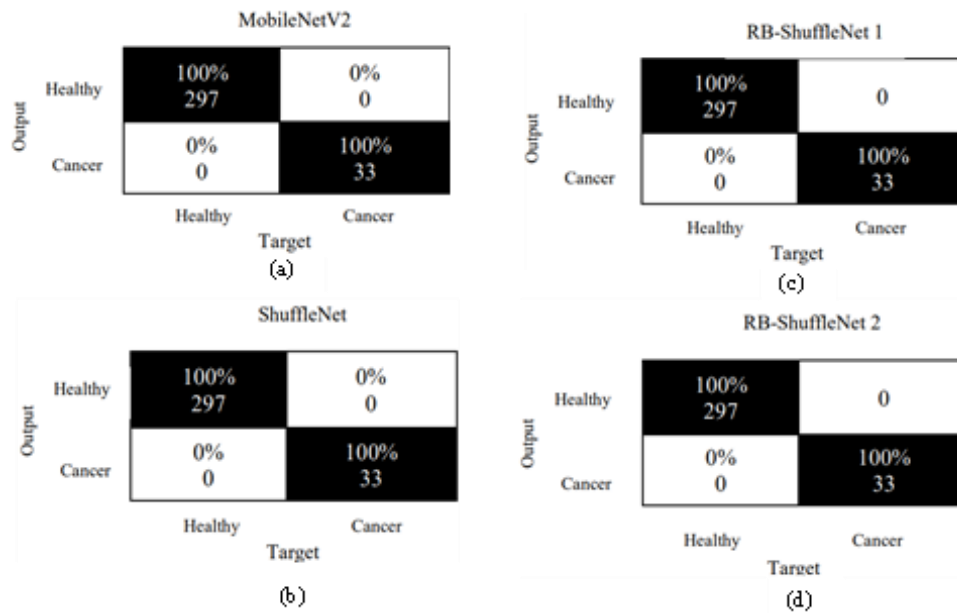


Figure 9. Confusion Matrix of (a) MobileNetV2, (b) ShuffleNet, (c) RB-ShuffleNet1, (d) RB-ShuffleNet2

3.3. Learning Parameters

Table 4 showed the learning parameters of all the models. These parameters are the number of weight and bias used to train the images. MobileNetV2 has the largest learning parameters, ShuffleNet has less than half MobileNets' parameters. While all RB-ShuffleNets have lesser learning parameters than MobileNetV2 and ShuffleNet. Fig. 10 illustrates the trade-off between classification accuracy and the number of learning parameters of the RB-ShuffleNet, MobileNetV2, and ShuffleNet. For mobile-based models, we need a network with the smallest number of learning parameters and the highest classification accuracy. If we look at Fig. 10, the blue dot (represent MobileNetV2), the red dot (represent ShuffleNet), and the green dots (represent the RB-ShuffleNet1 up to RB-ShuffleNet4) are the networks with 100% accuracy. However, the RB-ShuffleNets have fewer parameters worked the same capabilities as MobileNetV2 and ShuffleNet with more parameters. Thus, this new model is preferable for implementation on mobile devices. Smaller parameters lead to a faster training time.

Table 4. Learning parameter of the models

Model	Learnable Parameter
MobileNetV2	2.2M
ShuffleNet	0.86M
RB-ShuffleNet 1	0.70M
RB-ShuffleNet 2	0.54M
RB-ShuffleNet 3	0.39M
RB-ShuffleNet 4	0.35M
RB-ShuffleNet 5	0.30M
RB-ShuffleNet 6	0.26M
RB-ShuffleNet 7	0.22M
RB-ShuffleNet 8	0.18M

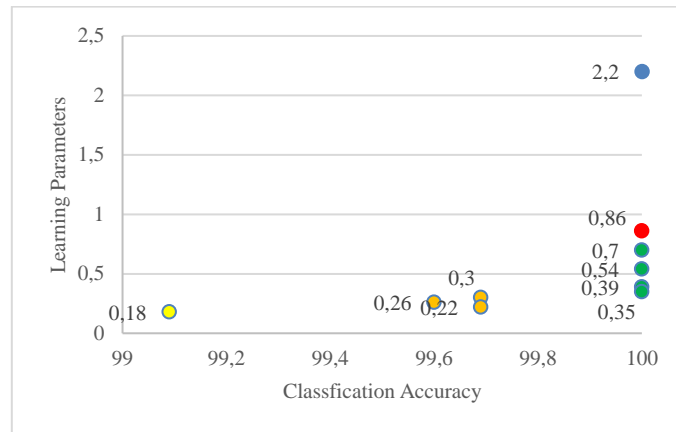


Figure 10. Trade-off between classification accuracy and number of learning parameters of RB-ShuffleNets, MobileNetV2, and ShuffleNet

3.4. Discussion

The ShuffleNet architecture has 50 layers, and the MobileNetV2 has 28 layers. However, the ShuffleNet has a channel-shuffle mechanism that made it possible to efficiently use its layers with smaller complexity than the MobileNetV2. This could accelerate the training time. Furthermore, the ShuffleNet has fewer learning parameters because the size of convolutional filters is different from MobileNetV2. Most of convolutional filters in the ShuffleNet is 1×1 , while MobileNetV2 is larger than it.

Research in [7] showed fine-tuning in ShuffleNet and MobileNetV2 to detect breast thermal images could increase the accuracy. They compared mobile-based deep learning models, ShuffleNet and MobileNetV2 with deep network like ResNet and DenseNet. The model was fine-tuned by using SGD, learning rate, and momentum value the same as we applied with lower epoch than our research. However, ShuffleNet still could not reach maximum accuracy to mobile-based deep learning. Other deep network like ResNet and DenseNet have been proven to obtain maximum accuracy in two classes of cases.

Study [5] implemented the segmented images before applying on CNN model. The segmented images have been done with curvature function and gradient vector flow. This method could extract only breast area and CNN could detect the cancer area on it. The segmented images contribute to increasing accuracy score.

The work in [16] analyzed some CNN architectures and reported that SqueezeNet, ShuffleNet, MobileNet, and NasNet-A-mobile are amongst CNN with the most efficient architecture for mobile applications. It was mentioned in the study that the density accuracy of SqueezeNet is lower than ShuffleNet. The work in [15] presented the comparison of the accuracy ShuffleNet and SqueezeNet in detecting COV-19, in which the accuracy of ShuffleNet was higher than that of SqueezeNet.

Based on the researches above, we used the same setting [7] on the model and added preprocessing before. We choose the simple technique to extract the breast area using intensity profile. This method has proved to segment the breast area by using the value of intensity. Moreover, we increased the epoch from [7] and ShuffleNet reached 100% of accuracy. Besides, we reduced the layer on ShuffleNet, which is RB-ShuffleNet to lighten the model while maintaining the accuracy. The result on RB-ShuffleNet reached maximum accuracy when using ROI images.

The effort to embed CNN architectures in mobile devices is increasing progressively. To the best of our knowledge, a study of how to embed the architecture efficiently has not been investigated. However, some efforts have already been attempted to reduce the learning parameters to suit the limited resources of mobile devices. A further study on efficient CNN-based mobile devices for health applications is challenging and useful.

4. CONCLUSION

In this paper, we proposed a reduced-block ShuffleNet (RB-ShuffleNet) for thermal breast cancer detection. We built eight architectures based on ShuffleNet, each with different number of reduced blocks. We trained and tested those RB-ShuffleNets with the images obtained from Database for Mastology Research (DMR). The images were first cropped based on the region of interest (ROI), in which the ROI is determined by using the red intensity profile. Both original and ROI images are also trained and tested using the ShuffleNet and MobileNetV2. The result showed that (1) The learning parameter of the RB-ShuffleNet is extremely lower than MobileNetV2, with comparable testing accuracy, (2) RB-ShuffleNet with up to four reduced blocks had less than 50% of the learning parameters of the original ShuffleNet, with maximum accuracy, (3) RB-

ShuffleNets resulted in higher accuracy when fed with ROI images, which means ROI + RBShuffleNet capable as ShuffleNet. However, ROI process added computation time, but it could reduce training time when using deep learning models. We recommended that RB-ShuffleNet is preferable to implement as one of mobile-based deep learning models in breast cancer detection, due to its light structure and good performance.

ACKNOWLEDGMENTS

Many thanks to Visual Lab, who provided datasets for our research.

REFERENCES

- [1] L. G. Falconí, M. Pérez, and W. G. A., "Transfer Learning in Breast Mammogram Abnormalities Classification With Mobilenet and Nasnet," in *International Conference on Systems, Signals and Image Processing*, 2019, pp. 109–114.
- [2] S. Guan, N. Kamona, and M. Loew, "Segmentation of Thermal Breast Images Using Convolutional and Deconvolutional Neural Networks," in *IEEE Applied Imagery Pattern Recognition Workshop (AIPR)*, 2018, pp. 1–7.
- [3] F. Javier, E. Santiago, Z. Fern, and J. Luis, "Detection of Breast Cancer Using Infrared Thermography and Deep Neural Networks," in *International Work-Conference on Bioinformatics and Biomedical Engineering*, 2019, pp. 514–523, doi: 10.1007/978-3-030-17935-9.
- [4] R. Roslidar *et al.*, "A Review on Recent Progress in Thermal Imaging and Deep Learning Approaches for Breast Cancer Detection," *IEEE Access*, vol. 8, pp. 116176–116194, 2020, doi: 10.1109/ACCESS.2020.3004056.
- [5] S. Tello-Mijares, F. Woo, and F. Flores, "Breast Cancer Identification via Thermography Image Segmentation with a Gradient Vector Flow and a Convolutional Neural Network," *J. Healthc. Eng.*, vol. 2019, pp. 12–19, 2019, doi: 10.1155/2019/9807619.
- [6] M. De Freitas Oliveira Baffa and L. Grassano Lattari, "Convolutional Neural Networks for Static and Dynamic Breast Infrared Imaging Classification," *Proc. - 31st Conf. Graph. Patterns Images, SIBGRAPI 2018*, pp. 174–181, 2019, doi: 10.1109/SIBGRAPI.2018.00029.
- [7] R. Roslidar, K. Saddami, F. Arnia, M. Syukri, and K. Munadi, "A study of fine-tuning CNN models based on thermal imaging for breast cancer classification," *Proc. Cybern. 2019 - 2019 IEEE Int. Conf. Cybern. Comput. Intell. Toward. a Smart Human-Centered Cyber World*, pp. 77–81, 2019, doi: 10.1109/CYBERNETICSCOM.2019.8875661.
- [8] H. Chougrad, H. Zouaki, and O. Alheyane, "Deep convolutional neural networks for breast cancer screening," *Comput. Methods Programs Biomed.*, vol. 157, pp. 19–30, 2018, doi: 10.1016/j.cmpb.2018.01.011.
- [9] J. Wang, B. Cao, P. Yu, L. Sun, W. Bao, and X. Zhu, "Deep learning towards mobile applications," *Proc. - Int. Conf. Distrib. Comput. Syst.*, vol. 2018-July, pp. 1385–1393, 2018, doi: 10.1109/ICDCS.2018.00139.
- [10] A. G. Howard *et al.*, "MobileNets: Efficient Convolutional Neural Networks for Mobile Vision Applications," 2017.
- [11] M. Sandler, A. Howard, M. Zhu, A. Zhmoginov, and L.-C. Chen, "Mobilenetv2: Inverted residuals and linear bottlenecks," in *Proceedings of the IEEE conference on computer vision and pattern recognition*, 2018, pp. 4510–4520.
- [12] X. Zhang, X. Zhou, M. Lin, and J. Sun, "ShuffleNet: An Extremely Efficient Convolutional Neural Network for Mobile Devices," in *Proceedings of the IEEE Conference on Computer Vision and Pattern Recognition (CVPR)*, 2018.
- [13] N. Ma, X. Zhang, H.-T. Zheng, and J. Sun, "Shufflenet v2: Practical guidelines for efficient cnn architecture design," in *Proceedings of the European conference on computer vision (ECCV)*, 2018, pp. 116–131.
- [14] F. N. Iandola, S. Han, M. W. Moskewicz, K. Ashraf, W. J. Dally, and K. Keutzer, "SqueezeNet: AlexNet-level accuracy with 50x fewer parameters and <0.5MB model size," pp. 1–13, 2016.
- [15] A. S. Elkorany and Z. F. Elsharkawy, "COVIDetection-Net: A tailored COVID-19 detection from chest radiography images using deep learning," *Optik (Stuttg.)*, vol. 231, no. January, p. 166405, 2021, doi: 10.1016/j.ijleo.2021.166405.
- [16] S. Bianco, R. Cadene, L. Celona, and P. Napolitano, "Benchmark analysis of representative deep neural network architectures," *IEEE Access*, vol. 6, pp. 64270–64277, 2018, doi: 10.1109/ACCESS.2018.2877890.
- [17] A. Howard *et al.*, "Searching for mobileNetV3," *Proc. IEEE Int. Conf. Comput. Vis.*, vol. 2019-October, pp. 1314–1324, 2019, doi: 10.1109/ICCV.2019.00140.
- [18] J. Zuluaga-Gomez, Z. Al Masry, K. Benagoune, S. Meraghni, and N. Zerhouni, "A CNN-based methodology for breast cancer diagnosis using thermal images," *Comput. Methods Biomech. Biomed. Eng. Imaging Vis.*, 2020, doi: 10.1080/21681163.2020.1824685.
- [19] S. Sushant, S. Anand, T. James, V. Aravind, and G. Narayanan, "Localization of an unmanned aerial vehicle for crack detection in railway tracks," *2017 Int. Conf. Adv. Comput. Commun. Informatics, ICACCI 2017*, vol. 2017-Janua, pp. 1360–1365, 2017, doi: 10.1109/ICACCI.2017.8126030.
- [20] R. Riantana, B. Arie, M. Adam, R. Aditya, Nuryani, and I. Yahya, "Early Detection of Breast Cancer by Using Handycam Camera Manipulation as Thermal Camera Imaging with Images Processing Method," *IOP Conf. Ser. Mater. Sci. Eng.*, vol. 176, no. 1, 2017, doi: 10.1088/1757-899X/176/1/012021.
- [21] W. Rawat and Z. Wang, "Deep convolutional neural networks for image classification: A comprehensive review," *Neural Comput.*, vol. 29, no. 9, pp. 2352–2449, Sep. 2017, doi: 10.1162/NECO_a_00990.
- [22] Y. Guo, Y. Liu, A. Oerlemans, S. Lao, S. Wu, and M. S. Lew, "Deep learning for visual understanding: A review," *Neurocomputing*, vol. 187, pp. 27–48, 2016, doi: 10.1016/j.neucom.2015.09.116.

- [23] K. Munadi et al., "A Deep Learning Method for Early Detection of Diabetic Foot Using Decision Fusion and Thermal Images," *Applied Sciences*, vol. 12, no. 15, p. 7524, Jul. 2022, doi: 10.3390/app12157524.
- [24] Grunau, Gilat, and Shai Linn, "Detection and Diagnostic Overall Accuracy Measures of Medical Tests." *Rambam Maimonides medical journal* vol. 9,4 e0027. 4 Oct. 2018

BIOGRAPHY OF AUTHORS



RIZKA RAMADHANA received the BCS degree in informatics in 2018, and the M.Eng degree in electrical engineering in 2021 from Universitas Syiah Kuala (Unsyiah). Her research interest is computer vision and image processing. Currently, she is working as a lecturer in Computer Science Department, Universitas Almuslim, Bireuen, Indonesia.



KHAIRUN SADDAMI received a B.Eng. degree in electrical engineering from Universitas Syiah Kuala (Unsyiah), Banda Aceh, Indonesia, in 2015, where he is currently pursuing a Ph.D. degree in the Postgraduate Program of Electrical and Computer Engineering and is also a Research Assistant with Multimedia and Signal Processing (MuSig) Research Group. His research interest is computer vision and image processing. Currently, he is working as a lecturer at Universitas Syiah Kuala, Banda Aceh, Indonesia.



KHAIRUL MUNADI received a B.Eng. degree from the Sepuluh Nopember Institute of Technology, Surabaya, Indonesia, in 1996, and the M.Eng. and Ph.D. degrees from Tokyo Metropolitan University (TMU), Japan, in 2004 and 2007, respectively, all in electrical engineering. From 1996 to 1999, he was with Alcatel Indonesia as a System Engineer. Since 1999, he has been with the Electrical and Computer Engineering Department, Universitas Syiah Kuala (Unsyiah), Banda Aceh, Indonesia, as a Lecturer, where he has been a Professor, since August 2019. He was a Visiting Researcher in information and communication systems engineering with the Faculty of System Design, TMU, from March 2007 to March 2008. He was also a Visiting Scholar with the Department of Computer Engineering, Suleyman Demirel University (SDU), Isparta, Turkey, in 2016. His research interests include multimedia signal processing, knowledge-based management, and disaster management. He is a member of the APSIPA



FITRI ARNIA received the B.Eng. degree from Universitas Sumatera Utara (USU), Medan, in 1997, the master's degree from the University of New South Wales (UNSW), Sydney, Australia, in 2004, and the Ph.D. degree from Tokyo Metropolitan University (TMU), Tokyo, Japan, in 2008. She has been with the Department of Electrical and Computer Engineering, Faculty of Engineering, Universitas Syiah Kuala (Unsyiah), since 1999. She was a Visiting Scholar with TMU, in 2013, and with Suleyman Demirel University (SDU), Isparta, Turkey, in 2017. Her research interests include signal, image, and multimedia information processing. She is a member of the ACM and APSIPA.